China Ocean Eng., Vol. 26, No. 4, pp. 653 – 668

DOI 10.1007/s13344-012-0049-6, ISSN 0890-5487

Numerical Simulation of Sloshing with Large Deforming Free Surface by MPS-LES Method*

PAN Xu-jie (潘徐杰), ZHANG Huai-xin (张怀新)[1] and SUN Xue-yao (孙学尧)

School of Naval Architecture, *Ocean and Civil Engineering*, *Shanghai Jiao Tong University*, *Shanghai 200030*, *China*

(Received 06 December 2010; received revised form 8 May 2012; accepted 13 July 2012)

ABSTRACT

Moving particle semi-implicit (MPS) method is a fully Lagrangian particle method which can easily solve problems with violent free surface. Although it has demonstrated its advantage in ocean engineering applications, it still has some defects to be improved. In this paper, MPS method is extended to the large eddy simulation (LES) by coupling with a sub-particle-scale (SPS) turbulence model. The SPS turbulence model turns into the Reynolds stress terms in the filtered momentum equation, and the Smagorinsky model is introduced to describe the Reynolds stress terms. Although MPS method has the advantage in the simulation of the free surface flow, a lot of non-free surface particles are treated as free surface particles in the original MPS model. In this paper, we use a new free surface tracing method and the key point is "neighbor particle". In this new method, the zone around each particle is divided into eight parts, and the particle will be treated as a free surface particle as long as there are no "neighbor particles" in any two parts of the zone. As the number density parameter judging method has a high efficiency for the free surface particles tracing, we combine it with the neighbor detected method. First, we select out the particles which may be mistreated with high probabilities by using the number density parameter judging method. And then we deal with these particles with the neighbor detected method. By doing this, the new mixed free surface tracing method can reduce the mistreatment problem efficiently. The serious pressure fluctuation is an obvious defect in MPS method, and therefore an area-time average technique is used in this paper to remove the pressure fluctuation with a quite good result. With these improvements, the modified MPS-LES method is applied to simulate liquid sloshing problems with large deforming free surface. Results show that the modified MPS-LES method can simulate the large deforming free surface easily. It can not only capture the large impact pressure accurately on rolling tank wall but also can generate all physical phenomena successfully. The good agreement between numerical and experimental results proves that the modified MPS-LES method is a good CFD methodology in free surface flow simulations.

Key words: *liquid sloshing*; *large deforming free surface*; *meshless*; *moving particle semi-implicit method* (*MPS*); *large eddy simulation* (*LES*)

1. Introduction

Liquid cargo ships are used to transport flammable or explosive cargo like petrochemicals or liquid natural gas over waterway from producers to users, so the safety of the liquid cargo hold needs to be evaluated carefully, and the primary concern is the loads induced by sloshing. Sloshing is the movement of liquid cargo in partially filled tank. When the ship is pitching, rolling or yawing, the liquid in hold will experience sloshing. When the excitation period is close to the intrinsic period of the

* This work was financially supported by the National Natural Science Foundation of China (Grant No. 50979059).
1 Corresponding author. E-mail: hxzhang@sjtu.edu.cn

liquid cargo in hold, the liquid will experience sloshing with violent free surface, and the violent free surface will cause severe impact pressure to the hold. Therefore it is necessary to predict the impact loads carefully on the design stage.

Liquid sloshing has been studied since the 1950's, and many analytical researches were performed. Lots of early studies of sloshing problems were performed with waves of low height, and the sloshing height was assumed to be sufficiently small so the nonlinear effects can be neglected. Graham and Rodriguez (1952) studied the impulsive and convective pressure in a rectangular container. Housner (1957) studied the pressure behavior of the response sloshing rectangular and cylindrical tank, and he divided the sloshing pressure into two components. The first component is the convective pressure caused by the sloshing of liquid in the tank, and the second component is the impulsive pressure due to the liquid acceleration in the tank. This idealization is a commonly applied formula for estimating the pressure in response sloshing rectangular and cylindrical tank. Abramson (1966) used the linear potential theory to study the sloshing phenomenon in cylindrical and spherical containers, and analyze the influence of tank which caused by changeable pressure with the predicted sloshing pressure.

After the 1970s, some experiments were implemented to investigate the pressure of liquid sloshing. Olsen and Johnsen (1975) did a series of experiments to study the maximum lateral force and wave elevation of a resonance sloshing tank. Strandberg (1978) conducted experiments to study the liquid sloshing pressure in a laterally oscillating tank. Rakeheja *et al*. (1991) experimentally measured the dynamic fluid sloshing pressure and its influence on the dynamic rolling stability of a partially filled tank. These experimental studies are very important parts of sloshing studies.

In the 1980s, the sloshing problem became an important issue in the design of the LNG tank. With the development of numerical technology, some numerical approaches were used to simulate the sloshing phenomenon. Nakayama and Washizu (1981) used the finite element and boundary methods to model the nonlinear sloshing, which is a two dimensional tank under horizontal and pitching periodic motions. Mikelis and Journee (1984) used the finite-difference solution with MAC approach to resolve free surface to study the sloshing behavior and its effect on ship motion.

In the 1990s, some new numerical technologies were used to study the sloshing problem. Hwang *et al*. (1992) used a boundary element method based on the plate method to study the phenomenon of three-dimensional sloshing. Armenio and Rocca (1996) used two methods to study the sloshing of water in rectangular open tank. The first method was the Reynolds Averaged Navier Stokes Equations (RANS), and the second was the Shallow Water Equation (SWE). In RANS, the free surface was simulated by a modified MAC method – SIMAC, compared with the experiment, and they found the RANS was more accurate than SWE, but in cases with large amplitudes, the SWE still could get good results. Carious and Casella (1999) analyzed lots of numerical methods in study of sloshing problem, including the finite element method, boundary element method, potential theory and the finite difference method, and in free surface traced method, VOF, MAC and so on are available.

In recent years, many new computational fluid dynamics methods have been developed to simulate the free surface flows including sloshing problem. Löhner *et al*. (2007) used the finite difference method to study the free surface flows including resonant sloshing simulations, and he used

unstructured mesh and VOF to trace the free surface. Yu (2007) used the finite difference method with level-set to trace the free surface to study the mixed sloshing of LNG tank. Delorme *et al*. (2009) used the SPH method to simulate the rolling of LNG tank, and results of SPH were compared with experiments.

Sloshing is a free surface flow problem, which is known to be difficult to use numerical simulation to calculate fluid fragmentation on free surface, and it is also difficult to handle complex geometries in a numerical simulation, so methods were proposed to handle the free surface, such as MAC, VOF and Level-set in mesh method, SPH and MPS in meshless method. Moving-Particle Semi-Implicit method (MPS) is a new fully Lagrangian meshless method which was proposed by Koshizuka *et al*. (1995) and Koshizuka and Oka (1996). Some ocean engineering problems have been studied by using MPS, including the motion of a floating body (Sueyoshi and Naito, 2001; Pan *et al*., 2008a), sloshing (Sueyoshi and Naito, 2001; Pan *et al*., 2008b; Pan and Zhang, 2008a), wave breaking (Gotoh and Sakai, 2006), pressure fluctuation in MPS (Hibi and Yabushita, 2004; Sueyoshi and Naito, 2002; Pan and Zhang, 2008b) and LES simulation in MPS (Gotoh *et al*., 2001). The MPS method has been demonstrated its advantage in simulation of free surface flow.

In practice, there are a large number of engineering problems belong to turbulent flow, and it is necessary to extend the original MPS method to the turbulent flow simulation. In the governing equations of Large Eddy Simulation, only Reynolds stress is a new term. So compared with the RANS, the governing equations of LES is easier to handle in MPS method.

The present research focuses on the simulation of sloshing with large deforming free surface. In this paper, the theory of MPS-LES is introduced firstly. Second, we introduce a new mixed free surface tracing method which can reduce the mistreatment of the non-free surface particles as free surface particles. Third, an area-time average method is introduced to reduce the pressure fluctuation in MPS. Then the MPS-LES method is applied to a 2D sloshing simulation.

2. MPS-LES Method

The MPS method was proposed by Koshizuka *et al*. (1995) and Koshizuka and Oka (1996), and the large-eddy simulation (LES) in MPS method was proposed by Gotoh *et al*. (2001). In Eulerian grid method, the Sub-Grid-Scale (SGS) model is used to address the turbulence issues, and in MPS method, however, grid is replaced by particles, so the model is called "Sub-Particle-Scale (SPS) model". As the same in the Eulerian LES, the SGS turbulence model is necessary in high Reynolds number flow simulation.

Details of original MPS method were also introduced by Pan *et al*. (2008a) and Pan (2009). For MPS-LES method, the velocity can be written as follows:

$$u_l = \overline{u}_l + u_l', \tag{1}$$

in which l is the spatial orientation, $\overline{u}_l$ is the particle scale component of u_l, and u_l' is the SPS turbulence component of u_l. So the continuity equation and the Navier-Stokes equations can be written as follows:

$$\frac{\partial \overline{u}_m}{\partial x_m} = 0 ; \tag{2}$$

$$\frac{\mathrm{D}\overline{u}_l}{\mathrm{D}t} = -\frac{1}{\rho}\frac{\partial \overline{p}}{\partial x_l} + \nu \frac{\partial^2 \overline{u}_l}{\partial x_m^2} + \overline{\boldsymbol{F}}_l + \frac{\partial}{\partial x_m}(-\overline{u'_l u'_m}); \ \frac{\mathrm{D}\overline{u}_l}{\mathrm{D}t} = \frac{\partial \overline{u}_l}{\partial t} + \frac{\partial}{\partial x_m}(\overline{u}_l \overline{u}_m) , \tag{3}$$

in which m is the other spatial orientation, ρ is the density of fluid, v is the kinematic viscosity, the parameter with $\overline{\ }$ means the dominant component of the original parameter, p is the pressure, and $\boldsymbol{F}$ is the body force vector. In Eq. (3) the Reynolds stress term is described by the Smagorinsky eddy viscosity model as follows:

$$-\overline{u'_l u'_m} = \nu_t \left(\frac{\partial \overline{u}_l}{\partial x_m} + \frac{\partial \overline{u}_m}{\partial x_l} \right) - \frac{2}{3} k \delta_{lm} , \tag{4}$$

in which ν_t is the kinematic eddy viscosity, k is the turbulent kinetic energy, and δ_{lm} is Kronecker's delta. The kinematic eddy viscosity and the energy dissipation can be written as follows:

$$\nu_t = C_\nu k^{1/2} \Delta ; \tag{5}$$

$$\varepsilon = \frac{C_\varepsilon k^{3/2}}{\Delta} , \tag{6}$$

in which C_v and C_ε are constant, and Δ is the initial distance of particles. By assuming the local turbulence appearance item is equal to the local turbulence dissipation item:

$$-\overline{u'_l u'_m} \frac{\partial \overline{u}_l}{\partial x_m} = \nu_t \left(\frac{\partial \overline{u}_l}{\partial x_m} + \frac{\partial \overline{u}_m}{\partial x_l} \right) \frac{\partial \overline{u}_l}{\partial x_m} = \varepsilon , \tag{7}$$

with Eqs. (4), (5), (6) and (7), the kinematic eddy viscosity can be written as follows:

$$\nu_t = (C_s \Delta)^2 \left[\frac{\partial \overline{u}_l}{\partial x_m} \left(\frac{\partial \overline{u}_l}{\partial x_m} + \frac{\partial \overline{u}_m}{\partial x_l} \right) \right]^{1/2} , \tag{8}$$

in which C_s is Smagorinsky constant, and the constant C_v in Eq. (5), constant C_ε in Eq. (6) and constant C_s in Eq. (8) should satisfy the following relation:

$$C_s^2 = C_\nu^{3/2} C_\varepsilon^{-1/2} , \tag{9}$$

and these constants are selected as: $C_v = 0.08$, $C_\varepsilon = 1.0$ and $C_s = 0.15$.

In this paper, 2D simulations are considered, so the partial differential of Reynolds stress term in Eq. (3) can be written as follows:

$$F_{spsx} = \frac{\partial}{\partial x}\left(2\nu_t \frac{\partial \overline{u}}{\partial x} - \frac{2}{3}k \right) + \frac{\partial}{\partial y}\left[\nu_t \left(\frac{\partial \overline{u}}{\partial y} + \frac{\partial \overline{v}}{\partial x} \right) \right]; \tag{10}$$

$$F_{spsy} = \frac{\partial}{\partial x}\left[\nu_t \left(\frac{\partial \overline{u}}{\partial y} + \frac{\partial \overline{v}}{\partial x} \right) \right] + \frac{\partial}{\partial y}\left(2\nu_t \frac{\partial \overline{v}}{\partial y} - \frac{2}{3}k \right), \tag{11}$$

in which F_{spsx} and F_{spsy} are x and y direction component of the partial differential of Reynolds stress term. In 2D simulation, the kinematic eddy viscosity can be written as follows:

$$\nu_t = (C_s \Delta)^2 P_r^{1/2} . \tag{12}$$

P_r in Eq. (12) is:

$$P_r = 2\left(\frac{\partial \overline{u}}{\partial x}\right)^2 + 2\left(\frac{\partial \overline{v}}{\partial y}\right)^2 + \left(\frac{\partial \overline{u}}{\partial y} + \frac{\partial \overline{v}}{\partial x}\right)^2 . \tag{13}$$

k in Eqs. (10) and (11) is:

$$k = \frac{C_v}{C_\varepsilon}\Delta^2 P_r . \tag{14}$$

The partial differential model in Eqs. (10), (11) and (13) is formulated in the following form:

$$< \frac{\partial f}{\partial x_l} >_i = \frac{\mathrm{d}}{n^0}\sum_{j\neq i}\left[\frac{f_j - f_i}{x_{lj} - x_{ij}} w\left(\left|\boldsymbol{r}_j - \boldsymbol{r}_i\right|\right)\right]. \tag{15}$$

in which f is any physical quantity, d is the number of space dimensions, n^0 is the initial particle number density, $\boldsymbol{r}$ is the coordinate vector of particles, and $w(\boldsymbol{r}_{ij})$ is the kernel function. In partial differential model, the kernel size is selected as $3.1l_0$ (Gotoh *et al*., 2001), and l_0 is the initial distance of particles.

3. Mixed Free Surface Traced Method

In MPS method, free surfaces are always clear as the result of the fully Lagrangian motion of particles, and particles in free surface have less neighbors as shown in Fig. 1, so if the particle's number density satisfies the following condition:

$$n_i^* < \beta n^0 , \tag{16}$$

where n^0 is the initial particle number density and n_i^* is the temporal number density of particle i, the particle is regarded as free surface particle and the pressure of this particle is 0 (p = 0). This is an initial condition for the pressure Poisson equation. β in Eq. (16) is suggested to be 0.8~0.99. n_i^* in Eq. (16) is needed for the calculation of the pressure Poisson equation (Pan *et al*., 2008a; Pan, 2009), while the simulation does not need any additional calculation for free surface tracing procedure, so it is efficient to use the original free surface tracing method of MPS to trace the free surface.

However, the original free surface tracing method of MPS will lead to some non-free surface particles being mistreated as free surface particle inevitably. In MPS simulation, the number density of particles which belong to the free surface is smaller than that of other particles (as shown in Fig. 1), so MPS theory uses the particle number density to find free surface particles. There are two sub-processes in an increment of time of MPS simulation. The first process is an explicit calculation step, and the second process is an implicit calculation step, and the free surface traced procedure is between these two calculation steps. At this stage, number density of particles is changed due to the first explicit calculation step, so most particles' β_i ($\beta_i = n_i^*/n^0$) are changed too, and some of them are smaller than 1.0, including fluid particles which do not belong to free surface. Those particles whose β_i is smaller than 1.0 will be treated as free surface particles and will be given 0 for initial pressure condition. In that case, particles which do not belong to free surface are mistreated (as shown in Fig. 2).

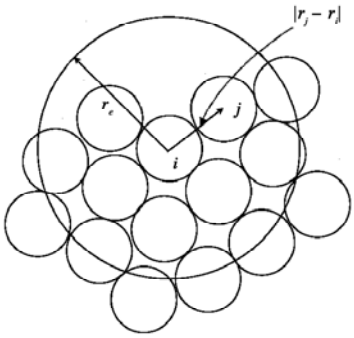

Fig. 1. Free surface particle and its neighbors.

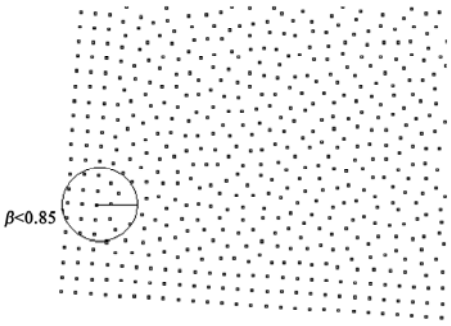

Fig. 2. Non-free surface particle mistreated as free surface due to β_i.

In this paper, a new free surface traced method is proposed, which is based on neighbors searching technology, and the search region is the same with Gradient model, so the simulation does not need any additional procedure, and the new free surface traced method can use the result of neighbors of Gradient model. In simulation, particles on the top layer of fluid can be treated as free surface, and particles near the free surface can be treated as the free surface too, so in the search method, $1.0l_0$~$2.1l_0$ of the Gradient model's region is considered, and this region is divided into eight parts. If two adjacent parts has no neighbors, the particle belongs to free surface, on the other hand, the particle does not belong to free surface (as shown in Fig. 3).

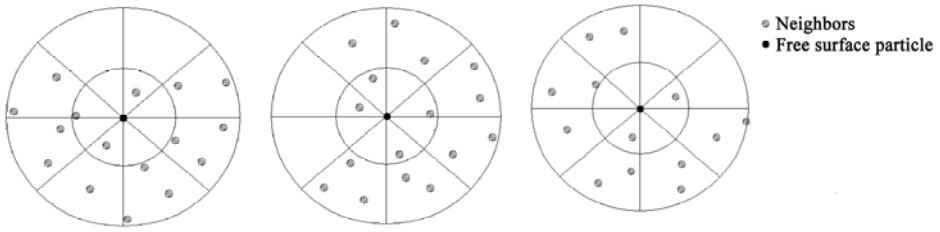

Fig. 3. Using neighbors for free surface.

But in the process of simulation, it is inefficient to use neighbors searching technology for each particle, especially when the case has a large number of particles. In fact, we do not need to check every particle in the simulation, and instead we can just use the neighbors searching technology to check the particles which are detected as free surface particle by Eq. (16) only. In some simulations, the splash phenomenon can take place in the free surface, then some particles belong to the free surface, but they have neighbors in eight separated parts. These particles will be mistreated as non-free surface particles if use the neighbors searching technology. In case of splash phenomenon, the distribution of particles is looser, and the number density of particle is relatively small. Then these particles can be treated as free surface particles directly. Therefore the neighbors searching approach is only applicable in the range of number density as follows:

$$D < \frac{n_i^*}{n^0} < \beta \,. \tag{17}$$

In Eq. (17), particles can be treated as non-free surface particles when β_i is bigger than β, and particles

can be deemed in the splash region when β_i is smaller than D, and these particles can be treated as free surface particles directly. β in Eq. (17) is suggested to be 0.97~0.99 which is the big value of β in the original free surface traced method of MPS. D in Eq. (17) is suggested to be 0.80~0.85 which is the small value of β in the original free surface traced method of MPS. But in some cases, simulations may have divergence because of the small value of D, so a bigger value of D can be selected in these cases.

4. Area-Time Average Method for Pressure Fluctuation

The value of pressure is very important for a numerical simulation, because serious pressure fluctuations always occur in MPS simulation, which has become an obstacle for the development of MPS method. Thus some studies are concentrated on the MPS pressure fluctuation phenomena. Hibi and Yabushita (2004) used different methods to reduce the pressure fluctuation. The first method is a new pressure equation for bottom particles which includes the hydrostatic pressure. The second method is a new anisotropic kernel function, and Hibi and Yabushita found that the kernel function links with the pressure fluctuation, and the anisotropic kernel function is better than a general kernel function. The third method is the double iteration of pressure Poisson equation. This method uses the double calculation of the first explicit calculation step to reduce the influence of pressure fluctuations. The fourth method is a new pressure Poisson equation.

These methods have a certain effect on the pressure fluctuation of MPS simulation. But these methods also bring defects in MPS simulation, because they are difficult to use, and they can make the MPS theory more complex.

Sueyoshi and Naito (2002) used a fixed time-area average method for pressure fluctuation, which comes from the real experiment. In the real experiment, the collection of pressure is based on the area and time average due to the area of pressure collector and the collection in a time period respectively. Result shows that the effect of the fixed area-time average is obvious, and the result of pressure is acceptable. Another advantage of this area-time average method is its easy application.

The main reason for pressure fluctuation is the particles' random movement. It can be found that the pressure of a particle depends on the particle's number density in the simulation (Pan *et al*., 2008a; Pan, 2009), and the number density counts on the distance between the particle and its neighbors. The distance of particles shows the randomness due to the random movement of particles, and thus the pressure of MPS is fluctuating. With numerous simulations (Pan *et al*., 2008a and b; Pan and Zhang, 2008a and b; Pan, 2009), we can find that although MPS can not guarantee the pressure of each time step close to the real pressure value, it can guarantee the average pressure in a time period close to the real value. So the MPS method can make a good simulation of the movement.

With consideration of the practicability and physics reason of MPS pressure fluctuation, the area-time average method is used in this paper for pressure fluctuation. In the area-time average method, the pressure is the area averaged and time episode averaged simultaneity before output. In this method, a restricted area around the pressure output particle is given, and the pressure of all particles in the restricted area is put out and averaged. In this paper, the pressure is averaged with the two closest neighbors of the pressure output particle because the simulation is 2D. Since the singular pressure may

be shown in the neighbor of the pressure output particle, this paper puts forward a weighted average method as follows:

$$(P_{i-1}+k\times P_i+P_{i+1}) / (k+2). \tag{18}$$

And in the time average method, the pressure is averaged in the chosen time episode, and the time episode is changed with the simulation period and time increment.

5. Numerical Simulation of Resonant Sloshing

Two numerical simulations of resonant sloshing have been carried out by using MPS-LES method, which combines the original MPS method with the mixed free surface traced method and the LES. Details of the numerical simulations are shown below:

(1) A rectangular tank sloshing in the horizontal direction;

(2) A modeled 2D LNG tank longitude section rolling in 2D plane.

5.1 Sloshing of A 2D Tank Due to Sway Excitation

The first example considers the sloshing of a partially filled 2D tank. The height and length of the tank are $L = H = 1$ m, and the filling level is $h = 0.35$ m. The details of the problem definition are shown in Fig. 4. Experimental data of this tank has been provided by Olsen and Johnsen (1975). In numerical simulation, Landrini *et al*. (2003) gave the result by using SPH method, and Löhner *et al*. (2007) gave the result by using VOF. In simulation, a wave gage is placed 0.05 m from the right wall, and the tank undergoes a sway motion. The tank oscillates horizontally and the law is:

$$x = A\sin(2\pi t / T), \tag{19}$$

in which x is the horizontal distance of the sloshing tank, A is the amplitude of the sloshing tank, and T is the sloshing period. The simulation lasts for 40 s, and all the output data are recorded in the last 10 s. Two amplitudes are chosen for the simulation, $A_1 = 0.025$ m and $A_2 = 0.05$ m. There are some natural periods for the liquid in tank, and the liquid in the tank will experience resonant sloshing when the excitation period is close to the natural period. The natural periods for the liquid in the tank can be calculated by the linear theory as follows:

$$f_m = \frac{1}{2}\sqrt{\frac{mg\cdot\tanh(m\pi h / L)}{\pi L}}, \tag{20}$$

where f_m is the resonant frequency of m-order, m is the order number, and g is the acceleration of gravity. With Eq. (20), it can be seen that the first resonant period of the liquid in the tank is $T_1 = 1.27$ s. Two series of simulation period based on T_1 are selected as shown in Tables 1 and 2.

Table 1 Different simulation periods for $A = 0.025$ m

T(s)	1.00	1.20	1.30	1.35	1.38	1.40	1.42	1.45	1.50	1.60	1.80
T/T_1	0.79	0.94	1.02	1.06	1.09	1.10	1.12	1.14	1.18	1.26	1.42

Table 2 Different simulation periods for $A = 0.05$ m

T(s)	1.00	12.0	1.30	1.35	1.40	1.43	1.45	1.47	1.50	1.60	1.65	1.70	1.75	1.80
T/T_1	0.79	0.94	1.02	1.06	1.10	1.13	1.14	1.16	1.18	1.26	1.30	1.34	1.38	1.42

As shown in Fig. 5 that the tank is assembled by 3357 particles. The distance of particles is l_0 = 0.0125 m, and the kernel function in the simulation is selected as follows:

$$w(r)=\begin{cases}1-6(r/r_e)^2+8(r/r_e)^3-3(r/r_e)^4, & 0\le r<r_e\\ 0, & r_e\le r\end{cases} \tag{21}$$

in which $r=r_j-r_i$, and r_e is the region of kernel function. In Eq. (17), D is 0.85 and β is 0.99. The output lateral force is averaged: the area is averaged by Eq. (18) and k = 5, and the time is averaged by 0.01 s which is equal to 1% of the shortest simulation period. The increment of time in the simulation is 0.0001 s.

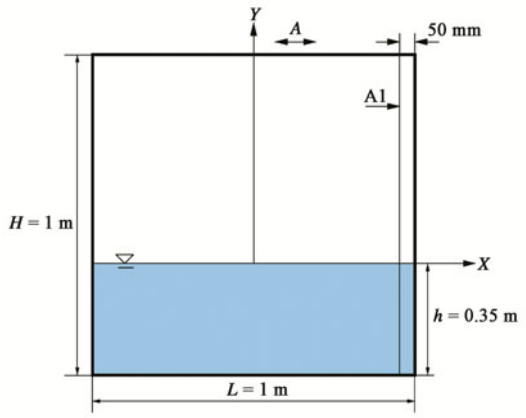

Fig. 4. Definition of sloshing 2D tank model.

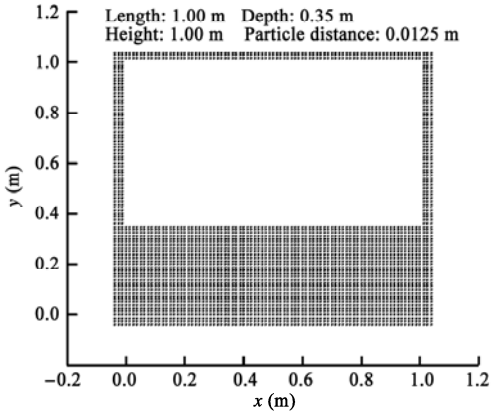

Fig. 5. Initial particles distribution of the sloshing 2D tank model.

The present MPS results are shown in Figs. 6 and 7. In Fig. 6a, the maximum wave elevation ζ at the wave probe A1 is compared with the experimental data, SPH results and VOF results for A/L = 0.025. In Fig. 6b, the maximum lateral force F_x at the right side of the tank is compared with VOF results for A/L = 0.025. In Fig. 7a, the maximum wave elevation ζ at the wave probe A1 is compared with the experimental data, SPH results and VOF results for A/L = 0.05. In Fig. 7b, the maximum lateral force F_x at the right side of the tank is compared with the experimental data, SPH results and VOF results for A/L = 0.05.

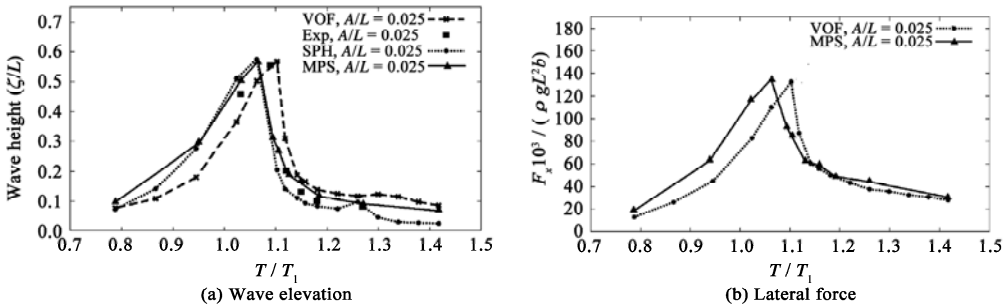

Fig. 6. Wave elevation and lateral force of simulations of A/L = 0.025.

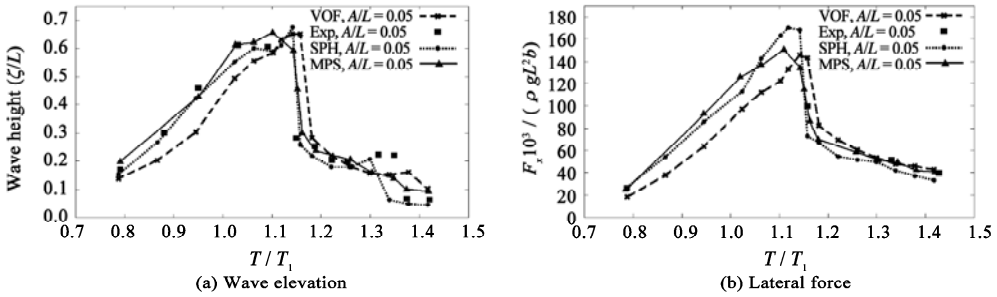

Fig. 7. Wave elevation and lateral force of simulations of A/L = 0.050.

Fig. 6 demonstrates the results when A/L = 0.025. It can be found from Fig. 6a that the maximum wave elevation predicted by MPS agrees with the experimental data, SPH results and VOF results, especially the SPH results. SPH is another Lagrangian particle method. In Fig. 6a, a small phase shift can be seen among the SPH, MPS results and VOF results, and the SPH and MPS results are closer to the experimental data when T/T_1 = 0.8~1.05, but VOF results are closer to the experimental data in resonant sloshing period. All numerical results are close to the experimental data when T/T_1 = 1.1~1.4. In Fig. 6b, only MPS and VOF results are demonstrated. Like the wave elevation result, a small phase shift can be found between the MPS and VOF results, but MPS results consist of VOF results in general.

Fig. 7 demonstrates the results when A/L = 0.05. In Fig. 7a, like results of A/L = 0.025, a small phase shift can be found among the SPH, MPS results and VOF results, but the shift is smaller than the results of A/L = 0.025, and all numerical results agree fairly well with the experimental data in wave elevation. In Fig. 7b, the lateral absolute values of the maximum force predicted by MPS are compared with SPH and VOF results. Although there is a small phase shift, all results agree with each other, but for the maximum value, SPH results are bigger than MPS and VOF results.

5.2 Sloshing of 2D LNG Tank Longitude Section Due to Roll Excitation

The second example considers the rolling of a partially filled 2D LNG tank longitude section, which is modeled with the scale 1:50, the length of the tank L = 90 cm, the height of the tank H = 54 cm, and the depth of filling d = 9.3 cm. Details of the problem definition are shown in Fig. 8.

Experimental data and SPH results of this tank have been provided by Delorme *et al*. (2009). The tank undergoes a rolling motion, and the rolling law is:

$$\theta = \theta_{\max} \sin(2\pi t / T), \tag{22}$$

in which θ is the angle of the rolling tank, $\theta_{\max}$ is the amplitude of the rolling tank, and T is the sloshing period. The simulation lasts for 15 periods, and the output position of pressure is on the wall, which is at the same level of free surface, and the maximum angle of the rolling tank is $\theta_{\max} = 4°$. According to Eq. (20), the first resonant period of the liquid in the tank is T_1 = 1.92 s, so that three simulation periods based on T_1 are selected as follows:

Case A: T_A = 2.112 s, T_A/T_1 = 1.1;

Case B: $T_B = 1.920$ s, $T_B/T_1 = 1.0$;

Case C: $T_C = 1.728$ s, $T_C/T_1 = 0.9$.

Fig. 9 shows that the tank is assembled by 3904 particles, and the distance of particles is $l_0 = 0.006$ m. The kernel function in simulation is selected below:

$$w(r) = \begin{cases} 2/3 - 4(r/r_e)^2 + 4(r/r_e)^3, & 0 \le r \le r_e/2 \\ 4/3 - 4(r/r_e) + 4(r/r_e)^2 - (4/3)(r/r_e)^3, & r_e/2 < r \le r_e \\ 0 & r_e < r \end{cases} \quad (23)$$

In Eq. (17), D is 0.94 and β is 0.98. The output lateral force is averaged: area averaged by Eq. (18) and k = 5, and time averaged by 0.015 s which is smaller than 1% of the shortest simulation period. The increment of time in the simulation is 0.0001 s.

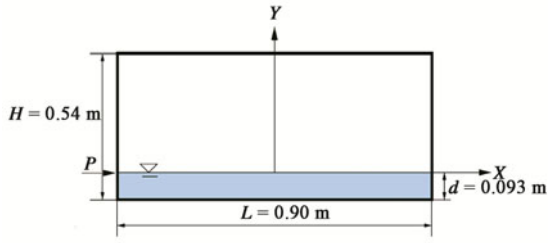

Fig. 8. Problem definition of the LNG tank longitudinal section.

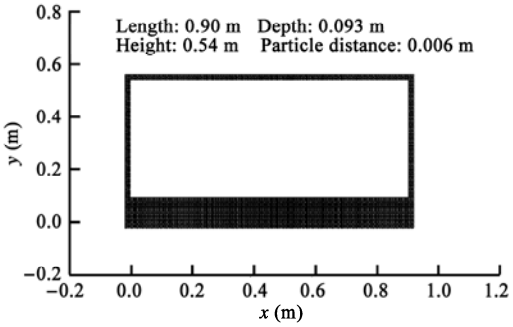

Fig. 9. Initial particles distribution of the LNG tank longitudinal section.

From Case A to Case C, the flow is composed of a main wave which travels from one side to the other side of the rolling tank. Some free surface snapshots are shown in Fig. 10. From Fig. 10, it can be found that the wave impacts the wall of the tank first, and then the water goes up along the wall. Different free surfaces are shown in snapshots. In Case C, the motion of the rolling tank is faster and the wave has more energy, so the breaking wave of Case C goes up higher than that of Case A and Case B. It means that the real resonant period of the liquid in the tank is $T_C = 1.728$ s, which is different from the theoretical resonant period $T_1 = 1.92$ s. The reason is that the simulations include nonlinearities, but the theoretical resonant period formula is derived from linear theory.

Fig. 11 shows the breaking event of a plunge-type breaker entrapping the air of Case B. In the experimental data, two water jets are formed successively as shown in Fig. 11a. In E1 of Fig. 11a, the first jet appears, and then it enters into the main wave in E2 of Fig. 11a, the second jet instantaneously appears in E4 of Fig. 11a, and then the jet impacts the water as shown in E5 and E6 of Fig. 11a. In numerical simulations, SPH and MPS methods reproduced these phenomena well, even of high nonlinearities, overturning waves are included. The second jet is clear in SPH simulation as E6 of Fig. 11b shows: the first jet is clearer in MPS simulation as E2 of Fig. 11c shows, and the second jet in MPS still can be found in E4 of Fig. 11c.

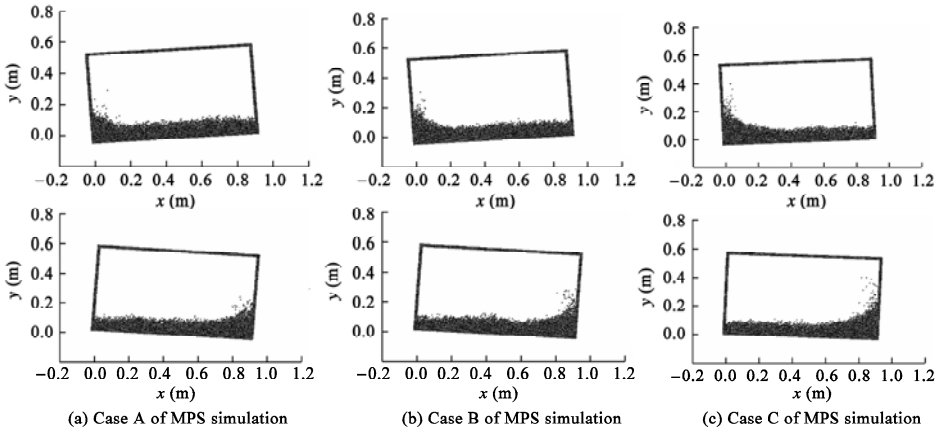

Fig. 10. Snapshots of free surface of simulations.

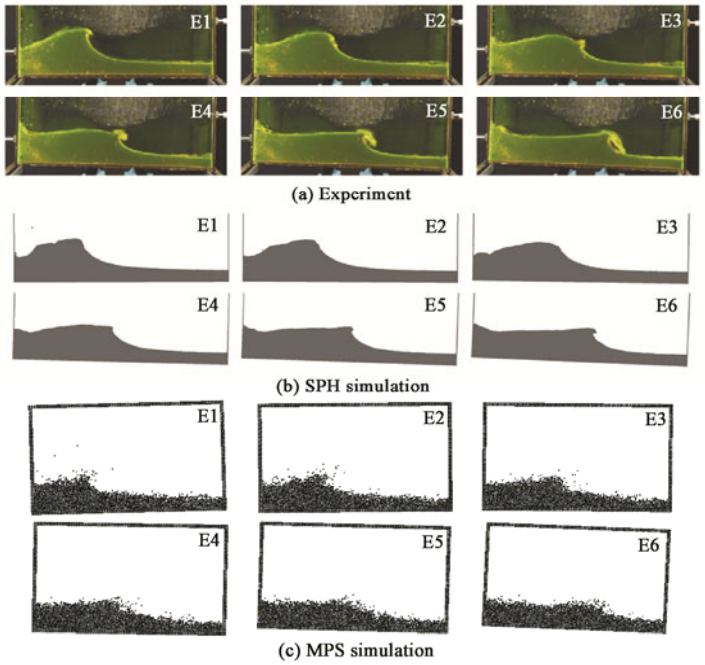

Fig. 11. Plunge-type breaking process of Case B.

Fig. 12 shows the details of the impact phenomena of Case B. With the rolling excitation, the main wave travels from one side to the other side. In F1 of Fig. 12a, the main wave is breaking just before the impact event. In F2 and F3 of Fig. 12a, the wave impacts the left wall and water runs up along the wall, and then the water falls down with the gravity and the tank wall's opposite movement, which is shown in F4 of Fig. 12a. Then the wave travels to the right wall as shown by F5 and F6 of Fig. 12a. In numerical simulations, results of SPH and MPS agree with the experiment well, and the free surface motion is well reproduced. But in the experiment, another wave travels behind the main

wave, which is shown in F3 of Fig. 12a. Since this secondary wave has lower energy, there is no impact event. In numerical simulation, the secondary wave is not very clear, but it still can be observed.

Dimensionless pressure of Case A, Case B and Case C is shown in Figs. 13a, 13b and 13c with the results of experiment, SPH simulation and MPS simulation respectively. Time has become dimensionless by the excitation period, as well as pressure has become dimensionless by the hydrostatic pressure at the reference depth. In pressure results of experiment, the random behavior can be found in impact pressure which is shown in Fig. 13a.

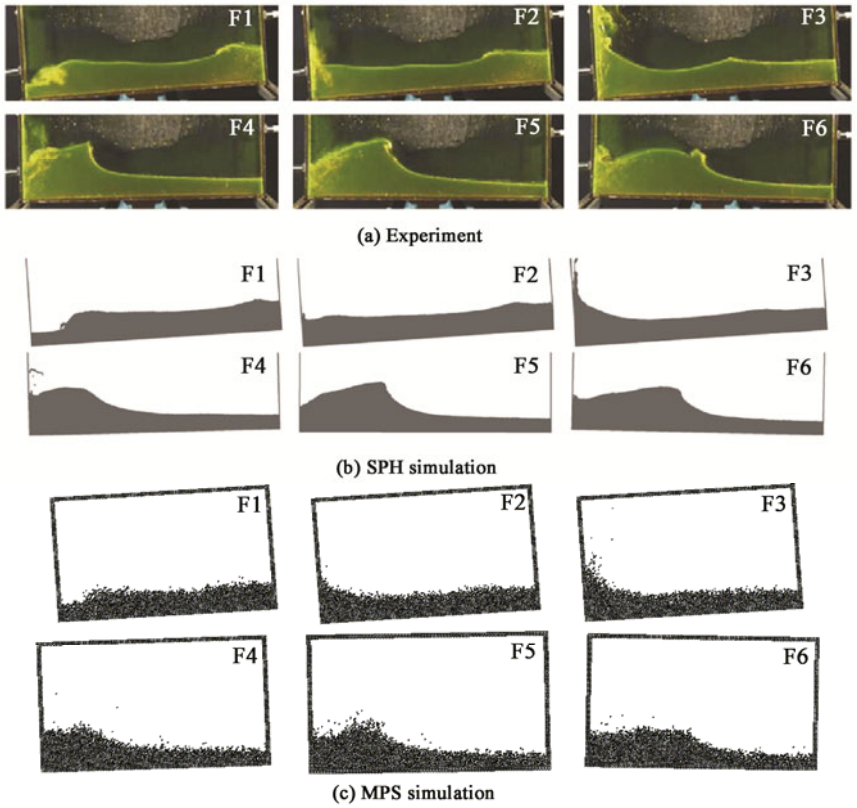

Fig. 12. Wave impact process of Case B.

This random behavior of pressure of experiment is caused by the free surface impact. As the impact time is very short and the impact pressure is sensitive to the shape of wave, and the impact pressure is rather instable. Pressure results of SPH and MPS shown in Figs. 13b and 13c agree with the experiment data generally, but in SPH results, the impact pressure is larger than the experiment one, while in MPS simulation, pressure results including the impact pressure are closer to the experiment data. Only in Case C, the impact pressure of MPS simulation is smaller than experimental data, and the difference between the impact pressure of experiment and MPS simulation may be caused by the average method for pressure or the random behavior of impact pressure.

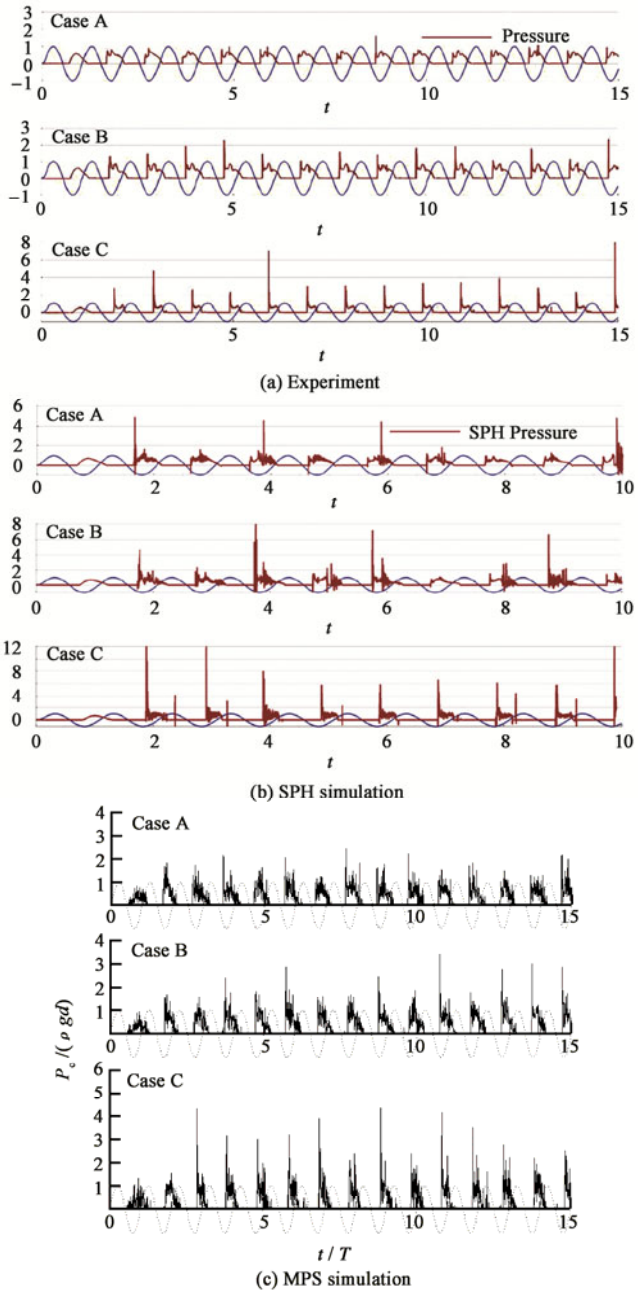

Fig. 13. Dimensionless pressure of Case A, Case B and Case C.

6. Conclusions

The MPS method is extended to the large eddy simulation (LES) by being coupled with a sub-particle-scale (SPS) turbulence model in this paper. A new mixed free surface traced method is

proposed for the mistreatment of non-free surface particles based on neighbors searching technique. This new method is of a high efficiency because we combine the new neighbors searching technique with the original search technique. For unacceptable pressure fluctuation of MPS method, an area-time average technique is used in this paper, and a weighted area average method is used for singular pressure.

Results show that these new technologies or methods are adapted to the MPS method and improved the original one. With these technologies, the modified MPS-LES method is good at the simulation of sloshing with large deforming free surface. The new mixed free surface traced method works well and reduces the mistreatment of free surface particles; different area-time average methods solve pressure fluctuation well, and the result of pressure is good and agrees fairly well with the results of experiments and other numerical methods.

References

Abramson, H. N., 1966. *The Dynamic Behavior of Liquid in Moving Containers*, NASA SP-106.

Armenio, V. and Rocca, L. M., 1996. On the analysis of sloshing of water in rectangular containers: numerical study and experimental validation, *Ocean Eng.*, **23**(8): 705~739.

Carious, A. and Casella, G., 1999. Liquid sloshing in ship tanks: a comparative study of numerical simulation, *Marine Structures*, **12**(3): 183~198.

Delorme, L., Colagrossi, A., Souto-lelesias, A., Zamora-Rodriguze, R. and Botia-Vera, E., 2009. A set of canonical problems in sloshing, Part I Pressure field in forced roll comparison between experimental results and SPH, *Ocean Eng.*, **36**(2): 168~178.

Gotoh, H., Shibahara, T. and Sakai, T., 2001. Sub-particle-scale turbulence model for the MPS method− Lagrangian flow model for hydraulic engineering, *Computational Fluid Dynamic Journal*, **9**(4): 339~347.

Gotoh, H. and Sakai, T., 2006. Key issues in the particle method for computation of wave breaking, *Coast. Eng.*, **53**(2-3): 171~179.

Graham, E. W. and Rodriguez, A. M., 1952. The characteristics of fuel motion which affect airplane dynamics, *Journal of Applied Mechanics*, **19**, 381~388.

Hibi, S. and Yabushita, K., 2004. A study on reduction of unusual pressure fluctuation of MPS method, *Journal of Kansai Society Naval Architects*, **241**, 125~131.

Housner, G., 1957. Dynamic pressure on accelerated fluid containers, *Bulletin of the Seismological Society of America*, **47**(1): 15~35.

Hwang, J. H., Kim, I. S., Seol, Y. S., Lee, S. C. and Chon, Y. K., 1992. Numerical simulation of liquid sloshing in 3-Dimensional tanks, *Computers and Structures*, **44**(1-2): 339~342.

Koshizuka, S., Tamako, H. and Oka, Y., 1995. A particle method for incompressible viscous flow with fluid fragmentation, *Journal of Computational Fluid Dynamics*, **4**(1): 29~46.

Koshizuka, S. and Oka, Y., 1996. Moving-particle semi-implicit method for fragmentation of incompressible fluid, *Nuclear Science and Engineering*, **123**(3): 421~434.

Landrini, M., Colagorossi, A. and Faltisen, O. M., 2003. Sloshing in 2D flows by the SPH method, *Proceeding of the 8th International Conference on Numerical Ship Hydrodynamics*, Busan, Korea, 1~15.

Löhner, R., Yang, C. and Oñate, E., 2007. Simulation of flows with violent free surface motion and moving objects using unstructured grids, *International Journal for Numerical Methods in Fluids*, **53**(8): 1315~1338.

Mikelis, N. E. and Journee, J. M., 1984. Experimental and numerical simulations of sloshing behavior in liquid tanks and its effect on ship motion, *National Conference on Numerical Methods for Transient and Coupled Problem*, Venice, Italy.

Nakayama, T. and Washizu, K., 1981. The boundary element method applied to the analysis of two-dimensional nonlinear sloshing problems, *International Journal for Numerical Methods in Engineering*, **17**(11): 1631~1646.

Olsen, H. A. and Johnsen, K. R., 1975. *Nonlinear Sloshing in Rectangular Tanks*: *A Pilot Study on the Applicability of Analytical Models*, Det Norske Veritas Report 74-72-S, vol. II.

Pan, X. J., Zhang, H. X. and Lu, Y. T., 2008a. Moving-particle semi-implicit method for vortex patterns and roll damping of 2D ship sections, *China Ocean Eng*., **22**(3): 399~407.

Pan, X. J., Zhang, H. X. and Lu, Y. T., 2008b. Numerical simulation of viscous liquid sloshing by moving-particle semi-implicit method, *Journal of Marine Science and Application*, **7**(3): 184~189.

Pan, X. J. and Zhang, H. X., 2008a. Moving-particle semi-implicit method for simulation of liquid sloshing on roll motion, *Journal of Shanghai Jiao Tong University*, **42**(11): 1904~1907.

Pan, X. J. and Zhang, H. X., 2008b. A study on the oscillations appearing in pressure calculation for sloshing simulation by using moving-particle semi-implicit method, *Chinese Journal of Hydrodynamics*, **23**(4): 453~463. (in Chinese)

Pan, X. J., 2009. *Moving-Particle Semi-Implicit Method Research and Application Based on Large Eddy Simulation*, Ph. D. Thesis, Shanghai Jiaotong University. (in Chinese)

Rakheja, S., Sankar, S., Ranganathan, R., Billing, J. R. and Mercer, W., 1991. Field testing of a tank truck and study of fluid sloshing, *Proceedings of International Truck & Bus Meeting & Exposition*, SAE paper 912679.

Strandberg, L., 1978. *Lateral Stability of Road Tankers*, VTI report 138A, National Swedish Road and Traffic Research Institute, Sweden.

Sueyoshi, M. and Naito, S., 2001. A study of nonlinear fluid phenomena with particle method (Part1), *Journal of Kansai Society Naval Architects*, **236**,191~198. (in Japanese)

Sueyoshi, M. and Naito, S., 2002. A study of nonlinear fluid phenomena with particle method (Part2), *Journal of Kansai Society Naval Architects*, **237**,181~186. (in Japanese)

Yu, K., 2007. *Level-Set RANS Method for Sloshing and Green Water Simulations*, Ph. D. Thesis, Texas A&M University.